Electron-energy-loss- and ultraviolet-photoemission-spectroscopy study of the VN_x system

W. K. Schubert, R. N. Shelton, and E. L. Wolf
Ames Laboratory, U.S. Department of Energy, Iowa State University, Ames, Iowa 50011
and Department of Physics, Iowa State University, Ames, Iowa 50011
(Received 1 December 1980)

Reflection electron-energy-loss spectroscopy (ELS) and ultraviolet-photoemission spectroscopy (UPS) have been used to study the electronic properties of VN_x ($0.0 \leq x < 0.96$). Polycrystalline samples of several compositions have been fabricated with special care to avoid oxygen contamination. ELS is used to examine the collective oscillations ("plasmons") of the valence electrons, and one-electron core-level excitations, while angle-integrated UPS experiments using the resonance lines of He and Ne are used to probe the valence-band density of states. The ELS experiments are the first of this type on any of the transition-metal nitrides or carbides, while the UPS results are the first reported for VN_x. Good overall agreement is found with the calculated density of states of Neckel *et al.* The experimental results seem to indicate that composition changes result in a reshaping of the hybridized $(V-3d)+(N-2p)$ valence band rather than a simple rigid-band–like shift of the Fermi level.

I. INTRODUCTION

The transition-metal nitrides and carbides (TMNC's) have long been of interest due to their unusual combination of physical properties.[1-3] These properties are closely tied to the electronic structure of the materials and have led to rather extensive theoretical[4-14] and experimental[15-21] investigations. TiC_x has been by far the most spectroscopically studied of the TMNC's. Early controversies[4,5] about the placement of the nonmetal $2p$ states and the associated direction of charge transfer have been resolved, favoring the results of augmented-plane-wave calculations of the band structure and the density of states (see Ref. 14 for a review of these calculations) which place the nonmetal $2p$ states below the Fermi level (E_F) and thus predict charge transfer from metal to nonmetal atoms.

The present work concentrates on the vanadium-nitrogen system which displays superconductivity[1,22-25] as well as the other properties commonly associated with the TMNC's. We have employed angle-integrated ultraviolet-photoemission spectroscopy (UPS) to investigate the valence-band density of states and reflection electron-energy-loss spectroscopy (ELS) to study the collective valence-electron oscillations and the core-level interband excitations. Samples of several compositions have been examined to determine the effects of the nitrogen-to-vanadium atomic ratio (x) on the electronic structure.

II. THE VANADIUM-NITRIDE SYSTEM

Although a complete phase diagram of the vanadium-nitride system is not available, it is well established that the superconducting δ-VN phase of VN_x lies in the composition range $0.72 \leq x \leq 1.00$.[1,22-25] The crystal structure in this range is the rocksalt structure ($B1$) with the vanadium atoms comprising an fcc lattice and the nitrogen atoms occupying octahedral interstitial sites. The lattice constant increases in a nearly linear fashion from $a_0 = 4.0662$ Å at $x = 0.72$ to $a_0 = 4.1398$ Å at $x = 1.00$.[22] Over this same composition range, the superconducting transition temperature increases from $T_c \approx 2$ K ($x = 0.72$) to $T_c \approx 9$ K ($x = 1.00$). This behavior is shown graphically in Fig. 1. Nitriding vanadium by directly heating the metal in nitrogen gas requires reaction temperatures above 1200 °C.[1]

A hexagonal phase, β-VN, exists for VN_x within the limits $0.35 \leq x \leq 0.49$.[1,22,23] β-VN is not a superconductor and is easily distinguished from δ-VN in x-ray diffraction measurements. A two-phase region of δ-VN and β-VN apparently exists for $0.49 \leq x \leq 0.72$.

III. EXPERIMENTAL

A. Sample preparation

The nature of the measurements employed in this study makes it imperative that samples of the highest possible purity and cleanliness be used. The major problem here is the avoidance of oxygen contamination, either in the bulk or on the surface. Bulk oxygen could degrade the superconducting T_c's while both bulk and surface oxygen would alter the UPS and ELS spectra. This latter problem turns out to be the most severe with VN. Samples of high bulk purity and displaying excellent T_c characteristics were sometimes unusable because an oxygen-free surface could not be obtained.

With this severe cleanliness restriction in mind, samples were fabricated by one of two techniques. The method we used most extensively involved nitriding the vanadium *in situ*. A major advantage here is the stringent control over the nitriding environment. An electropolished, high-purity (99.99%) vanadium foil (~ 0.08 mm thick) was cleaned in acetone and methanol before being

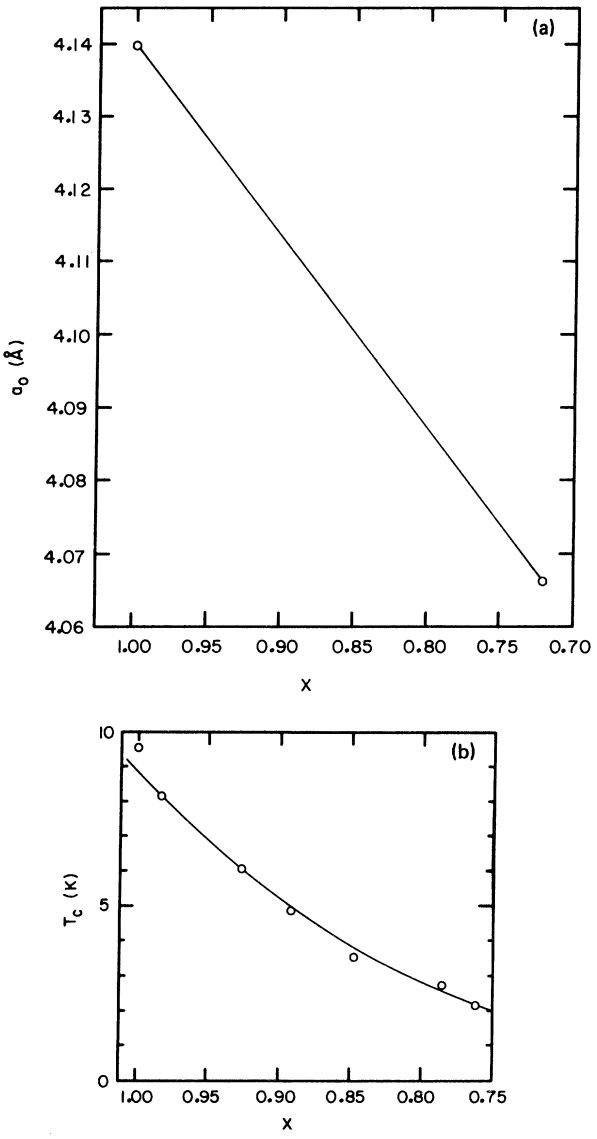

FIG. 1. (a) Dependence of the lattice constant on the N/V ratio (x) (Ref. 22). (b) Dependence of the superconducting transition temperature on the N/V ratio (Ref. 1).

placed in the ultrahigh vacuum (UHV) chamber. After reaching a base pressure of $\leq 1.0\times10^{-10}$ Torr the vanadium-foil surface was made atomically clean through extensive high-temperature outgassing ($\lesssim$1600 °C at $< 1\times10^{-9}$ Torr) followed by several cycles of sputter cleaning (3-keV Ar^+ ions) and lower-temperature (~ 1000 °C) annealing. This procedure leaves a foil that shows no contamination in the Auger electron spectra, but displays some evidence of oxygen $2p$ states in the UPS spectra. After obtaining a clean vanadium foil, the UHV chamber was sealed and filled with nitrogen (99.999%) to a pressure of 0.0 atm $< P \lesssim 1.0$ atm through a Varian leak valve, connected by a previously baked stainless-steel line directly to the gas cylinder. Alternating current through the vanadium foil was used to heat it to temperatures $\geq$ 1200 °C (as measured with an optical pyrometer) for up to 15 hours. Finally, the nitrogen was removed and UHV restored for the spectroscopic measurements.

The disadvantages of the *in situ* method are that one has no foreknowledge of the sample nitrogen content (and thus the T_c or even the crystal structure) and that there are difficulties in producing homogeneous samples. Nitriding temperatures and pressures play an important role in determining the final composition and the homogeneity. These parameters are rather poorly controlled in the *in situ* method.

In an attempt to overcome these problems of the *in situ* techniques, some samples were also fabricated externally using more conventional means. UHV-cleaned rectangles ($10\times20\times0.08$ mm^3) of vanadium foil were wrapped successively in foils of molybdenum, zirconium, and tantalum and then placed in a 3-in.-diameter mullite tube furnace. The wrappings were intended to provide extra protection against oxygen contamination during nitriding. Nitrogen flow rates varied from 50 to 100 cm^3/min and nitriding temperatures from 1200 to 1450 °C were used. The prepurified nitrogen gas was further cleaned by passing it initially through a drying column and an 800 °C gettering oven filled with copper mesh and zirconium foil. This method is quite similar to that reported by Ajami and MacCrone[26] except some extra precautions have been taken to avoid oxygen contamination. Apparently due to the protective wrappings, our nitriding times had to be increased by roughly 100 times over those reported in this earlier study to obtain homogeneous samples. The average nitrogen content of these samples was determined nominally by measuring the mass increase due to the nitriding. This resulted in compositions in agreement with those determined from the lattice-constant dependence on N/V shown in Fig. 1.

The major problem with the externally made samples was the oxide layer which grew when the samples were (necessarily) exposed to air. Due to this oxide layer (determined from depth profile measurements to be tens of angstroms thick), the externally made samples required extensive surface cleaning procedures when mounted in the UHV chamber. It has been reported for TiC and TiN by Johansson *et al.*[19] that repeated flash heating to high temperatures provided clean surfaces without altering the surface nonmetal-to-metal ratio. We found this method unsatisfac-

TABLE I. Results of characterizations by x-ray diffraction and ac inductive transition-temperature measurements.

Sample	Nit. time (h)	Nit. press. (atm)	Nit. temp. (°C)	a_0(Å)	x	T_c(K)	ΔT_c(K)[a]	% of sample[b]
VN-2	1	0.001	1300		β-VN			
VN-4	1	0.02	1500	4.077	0.76	4.5	2.0	100
VN-5	1	0.05	1530	4.088	0.80	8.35	0.4	30
						4.9	0.9	70
VN-6	1	0.10	1560	4.098	0.84	8.22	0.7	65
						5.68	0.5	35
VN-7	3	0.40	1560	4.101	0.85	8.4	0.4	30
						6.1	0.6	70
VN-9	7	0.8	1450	4.119	0.92	7.8	0.9	100
VN-10[c]	15	0.8	1230	4.123	0.94	8.4	1.4	100
VN-11	14.5	1.0	1330	4.125	0.94	8.25	0.7	45
						5.4	1.5	55
VN-*F*6	106	50 cc/min	1220	4.129	0.96	8.65	0.3	65
						5.4	2.3	35

[a] ΔT_c is the superconducting transition width as determined from 10% complete to 90% complete.

[b] % of sample is estimated from the relative height of the steps in the inductive T_c curves as measured on finely ground powders. Note that since no sample other than VN-10 gave indication of other than a single phase or composition from careful x-ray measurements, these numbers may overestimate the amount of competing phase present. See text for details.

[c] Sample VN-10 showed ≲5% β-VN in the x-ray diffraction pattern.

tory for VN, apparently due to its lower decomposition temperatures. We have found that sputter cleaning with argon ions at room temperature, followed by further sputtering at temperatures ≲ 1200 °C, and followed finally by annealing at ~ 1000 °C is required to provide clean VN surfaces without continually depleting the nitrogen content.

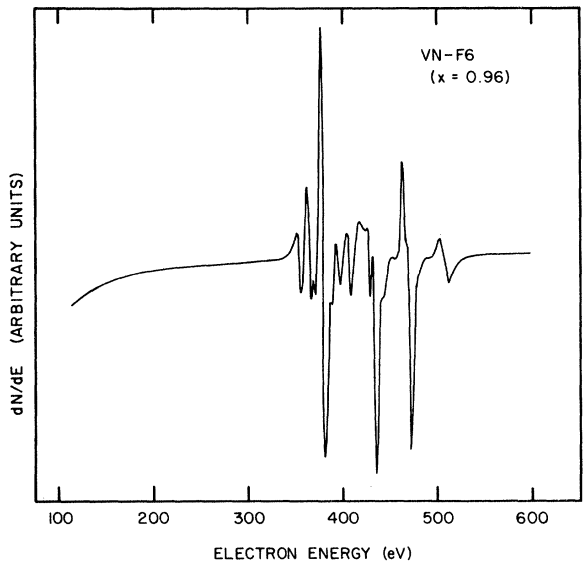

FIG. 2. Typical Auger electron spectrum for a clean δ-VN sample. Note there is no evidence of the carbon peak at ~270 eV. The oxygen and vanadium Auger spectra overlap around 500 eV, but this trace shows little or no oxygen contribution.

During both UPS and ELS measurements, the sample surface cleanliness was monitored using Auger electron spectroscopy (AES). Periodic (approximately every 15 min.) outgassing to 1000 °C was required to maintain clean surfaces. A typical Auger spectrum for a VN_x sample is shown in Fig. 2.

B. Sample characterization

All samples described here have been characterized by both x-ray diffraction and ac inductive transition-temperature measurements. This is necessary because the superconducting properties are critically related to the nitrogen content, the impurity levels, the crystal structure, and the sample homogeneity. The results of these characterizations, along with the sample preparation parameters are shown in Table I.

The lattice constant and composition range of δ-VN found in this study agree well with those reported in the literature.[1,22-25] The x values shown in Table I are determined from the lattice constant. It should be noted that several of the samples listed in Table I showed multistructured transition-temperature curves, suggesting the

existence of regions of different composition, even though x-ray diffraction results showed well resolved Cu $K\alpha_1$ and $K\alpha_2$ doublets and a single lattice constant and hence good homogeneity. The T_c measurements were done on finely powdered specimens to avoid shielding effects that could overestimate the contribution from a thin surface layer. We have been unable to determine a consistent and complete explanation for this phenomenon. Because of the possibility of incomplete homogeneity, these particular samples should not be relied upon too heavily in looking for compositional dependences. Their ELS and UPS spectra are, however, certainly representative of δ-VN. Samples VN-4 ($x = 0.76$) and VN-9 ($x = 0.92$) show suitably sharp diffraction patterns and homogeneous T_c's so that they can be used for studying compositional comparisons. VN-10 shows fairly good T_c results but contains a very small (< 5%) amount of β-VN impurity phase. We will rely primarily upon these three samples for our study of compositional dependences.

C. ELS and UPS measurements

The UHV apparatus used in these experiments, which has a base pressure $\leq 10^{-10}$ Torr, has been described elsewhere.[27] A two-stage cylindrical mirror analyzer (CMA) was used for AES, ELS, and UPS measurements. A grazing-incidence electron gun was used for AES and ELS while a microwave-excited noble-gas discharge lamp[28] was used in UPS experiments. The foil samples are mounted in stainless-steel clamps attached to a precision manipulator.

ELS measurements were taken as outlined in previous work.[27] Unless otherwise noted, all ELS spectra shown here were obtained using 500-eV primary electrons. Peak-loss values obtained at other primary energies yielded identical results. First-derivative spectra $[dN(E)/dE]$ are used to locate core-level thresholds while the negative second derivative $[-d^2N(E)/dE^2]$ is used to examine the collective oscillations. The undifferentiated loss spectra $N(E)$ are used primarily for looking at loss intensities. The resolution in the ELS measurements is limited by the full width at half maximum (FWHM) of the primary beam. This width improves from ~ 0.7 eV at $E_p = 1000$ eV to ~ 0.4 eV at $E_p = 100$ eV.

The angle-integrated photoelectron energy distribution curves (EDC's) were recorded using He I (21.2 eV), He II (40.8 eV), Ne I (16.8 eV), and Ne II (26.9 eV) ionization lines. Note that the Ne II EDC also shows a contribution from the fairly intense satellite line at 27.6 eV. To sustain the low-pressure discharge (~ 10 Torr) required for the second ionization lines, a weak axial magnetic field was applied to the discharge capillary.[29] The instrumental resolution can be estimated from the sharpness of the Fermi edge in VN and appears to be ~ 0.4 eV with a CMA pass energy of 25 eV.

IV. RESULTS AND DISCUSSION

A. ELS

Typical ELS spectra for V and δ-VN are shown in Fig. 3. We are unaware of any previous ELS work on any of the TMNC's. A detailed discussion of the vanadium spectra has been published previously.[27]

The following comparisons between V and δ-VN should be noted in the core-level region (energy losses $\gtrsim 30$ eV). The V $3p$ and V $3s$ core levels [located by peaks in $dN(E)/dE$] have shifted to greater binding energies in the nitride (36.6 eV → 39.9 eV for V $3p$ and 66.9 eV → 68.0 eV for V $3s$). This shift is consistent with, but not proof of, charge transfer from the vanadium atoms to the nitrogen atoms. The additional structure, extending roughly 25 eV beyond the V $3p$ level in both V and δ-VN, has changed shape in the nitride. This additional structure (observed in many of the transition metals and their compounds[27]) is believed to be related to the empty final states just above E_F, but is not completely understood for the early members of the third-row transition metals.[30,31] However, one would anticipate the alteration due to the hybridization of the V $3d$ and N $2p$ states near E_F in VN.

In the collective region (energy losses ≤ 30 eV), changes caused by nitriding are more dramatic. The free-electron-like volume and surface collective oscillations ("plasmons") of the valence electrons have shifted from 21.5 eV and 14.8 eV in V to ~ 25.3 eV and ~ 15.3 eV in δ-VN. The calculated free-electron "plasmon" energies (using the valence electrons) predict this shift fairly well for the volume contribution (22.3 eV for V and 24.9 eV for $VN_{1.00}$ using the V $3d$ and N $2p$ electrons). δ-VN also shows a shoulder to the volume plasmon in $-d^2N/dE^2$ which is of unknown origin. The so-called "lowered plasmons" observed in vanadium (and other transition metals[27,32,33]) at 9.6 eV (volume) and 5.3 eV (surface) seem to persist in δ-VN, also shifting to higher energies (~ 10.8 and ~ 7.0 eV, respectively). In addition to these collective oscillations, one observes the appearance of a very sharp low-energy peak at 2.8 eV in the nitride that was not present in V. Preliminary work on other transition-metal nitrides (NbN and ZrN indicate this low-energy peak

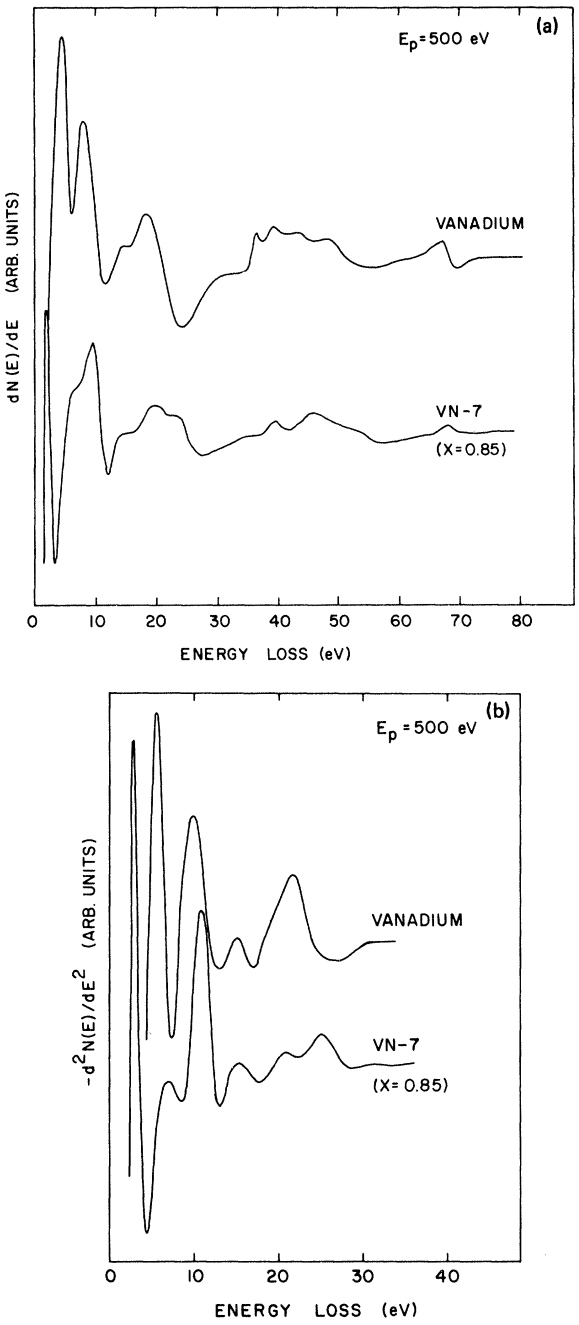

FIG. 3. (a) ELS dN/dE spectra for pure vanadium and a δ-VN sample. The vanadium $3p$ and $3s$ core levels can can be seen at $\lesssim 40$ and $\lesssim 70$ eV, respectively. The core levels shift to greater binding energy in the nitride. (b) ELS $-d^2N/dE^2$ spectra for pure vanadium and a δ-VN sample.

may be characteristic of ELS spectra from these materials. This low-energy peak could be caused by interband transitions near the Fermi level.

Figure 4 shows the dependence of the energy-loss intensities on the primary energy E_p. The light vertical lines mark the loss energies as determined by dN/dE and $-d^2N/dE^2$ for $E_p = 500$ eV. The intensity dependence on E_p is helpful in distinguishing surface from volume contributions in the loss spectra. Generally, volume contributions are expected to be more prominent at higher primary energies while surface contributions should dominate at lower energies. No attempt has been made to remove the multiple scattering background (which becomes quite evident in the $E_p = 100$ eV spectrum). Note the improved resolution of the low-energy (2.8 eV) peak as E_p decreases, due to reduction of the energy width of the primary beam. The intensities for the core-level excitations at ~ 39.6 and ~ 68.0 eV seem to decrease with primary energy (probably a cross-sectional dependence). Intensity changes with E_p in the collective region provide some evidence for the volume nature of the ~ 25-eV peak in that its relative intensity seems to decrease with E_p.

Our identification of the plasmon energies must be considered tentative since the detailed behavior of the real and imaginary parts of the complex dielectric function cannot be readily deduced from our reflection ELS data. However, the correspondences with the vanadium spectra, the good agreement with the free-electron plasmon calculation, and the demonstrated volume nature of the 25.3-eV peak give us reasonable confidence in our assignments.

Efforts to determine compositional dependences in the ELS spectra are shown in Fig. 5 and the loss values (including some samples not shown in Fig. 5) are given in Table II. The spectra represent samples covering most of the stable δ-VN composition range, as well as pure V and a V_2N sample (β-VN). As mentioned above, VN-4, VN-9, and VN-10 should be used primarily for these comparisons due to homogeneity requirements.

The β-VN sample is easily distinguished from the δ-VN samples in the collective region. However, for those samples within the δ phase, no obvious x-dependent trends are seen. Within the free-electron plasmon calculation, the change in valence-electron density should cause an increase of the volume plasmon energy by ~ 0.7 eV on increasing x from 0.72 to 1.00. This type of behavior has been observed in optical experiments by Lynch *et al.*[21] on TiC_x. We see no trends of this type, but they may be obscured by the relatively low resolution of our experiment. Small monotonic core-level shifts (of about 0.2 eV) have been observed by Johansson *et al.*[15] in TiC_x as x increases. Although we see a ~ 1.0-eV shift between V and δ-VN (for the V 3s core level), no trends within the δ phase are observed (again, our resolution may be too low).

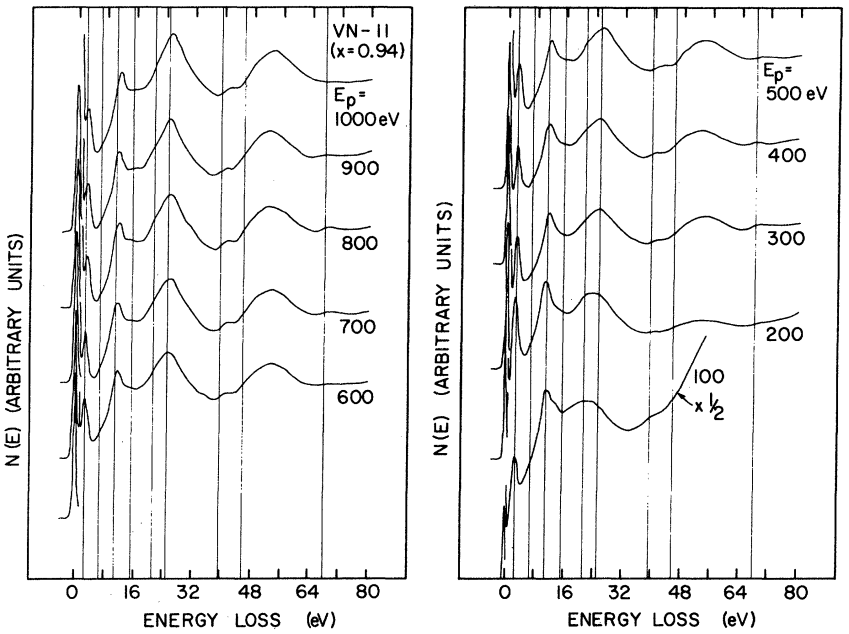

FIG. 4. ELS $N(E)$ spectra at several different primary energies (E_p) for a δ-VN sample. Volume contributions should dominate at larger E_p values. The light vertical lines mark the loss values determined by dN/dE and $-d^2N/dE^2$ for E_p =500 eV. The curves are normalized with respect to the primary peak intensity at 0 eV which is shown reduced in gain by 33.3 times.

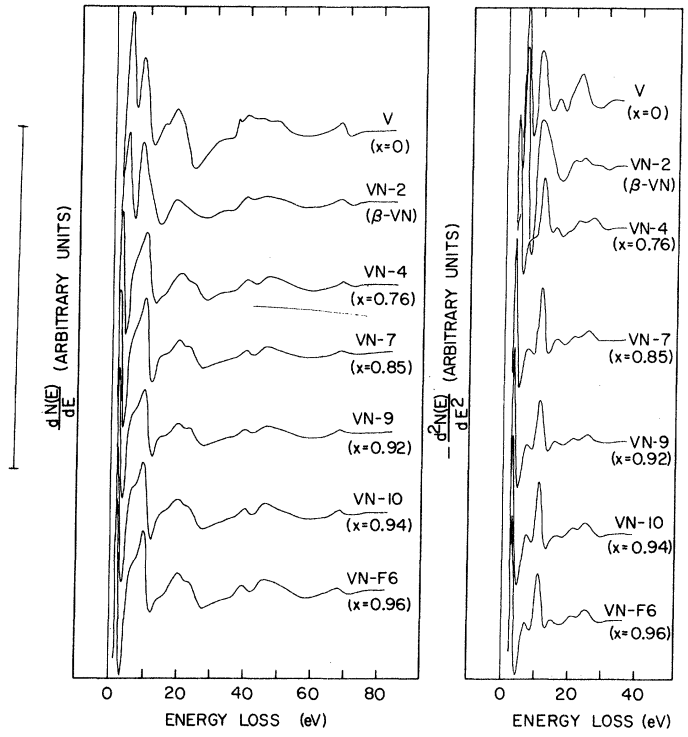

FIG. 5. (a) ELS dN/dE spectra for samples of several different compositions taken at E_p =500 eV. (b) ELS $-d^2N/dE^2$ spectra for samples of several different compositions taken at E_p =500 eV.

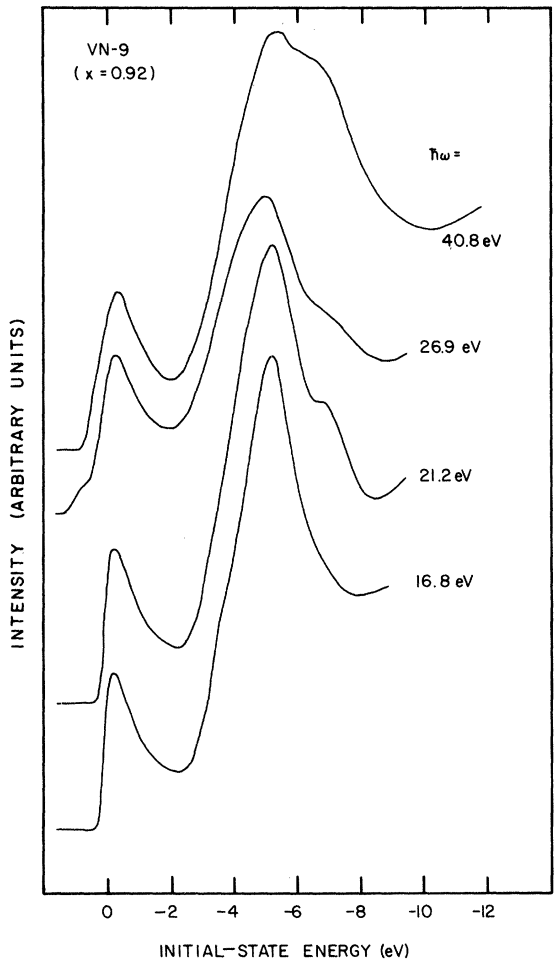

FIG. 6. Photoemission EDC's for a VN sample taken at several photon energies. The spectra are normalized with respect to the peak near E_F. The resolution decreases for $\hbar\omega = 26.9$, 40.8 eV because the cylindrical mirror analyzer (CMA) pass energy was increased to offset smaller signal strengths. The shoulder above E_F and the broadening of the left side of the −5.0-eV peak in the 26.9-eV curve are due to a neon satellite line at 27.6 eV.

B. UPS

EDC's for $VN_{0.92}$ at $\hbar\omega = 16.8$, 21.2, 26.9, and 40.8 eV are shown in Fig. 6. Note that the resolution decreases in the 26.9- and 40.8-eV spectra because the CMA pass energy was increased to offset the reduced signal strengths. Note also that the shoulder above E_F and the increased width on the low-energy side of the second peak (− 5.2 eV) is due to the 27.6-eV Ne satellite line. The calculated density of states (DOS) of Neckel *et al.*[10] is shown for comparison in Fig. 7. Agreement with the calculated DOS is fairly good with respect to the hybridized (V 3*d*) + (N 2*p*) bandwidth (~ 8.5 eV) and the general shape. Experimental peaks

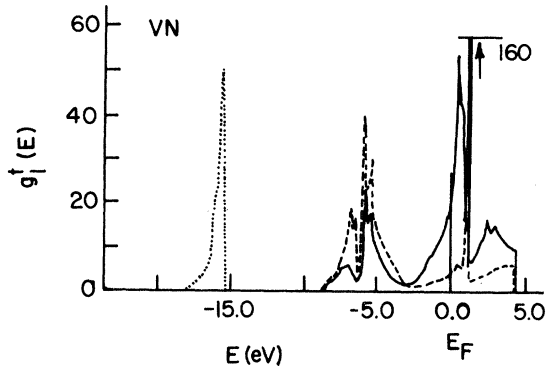

FIG. 7. The calculated density of states for stoichiometric VN of Neckel *et al.* (Ref. 10). The solid line represents V 3*d* states, the dashed line represents N 2*p* states, and the dotted line corresponds to the N 2*s* electrons.

and minima lie somewhat closer to E_F than in the calculation.

Both photon energy and angular dependences are observed in the region from − 2.5 to − 8.5 eV. The shoulder at − 7.0 eV grows in intensity as $\hbar\omega$ increases, possibly reflecting an increase in the N 2*p* photoexcitation cross section, since the calculation reveals this shoulder is primarily of N 2*p* character. UPS measurements on TiN (a material which possesses a very similar DOS[10]) by Johansson *et al.*[19] show this same intensity behavior. Although we report angle-integrated measurements, Fig. 8 shows some residual angu-

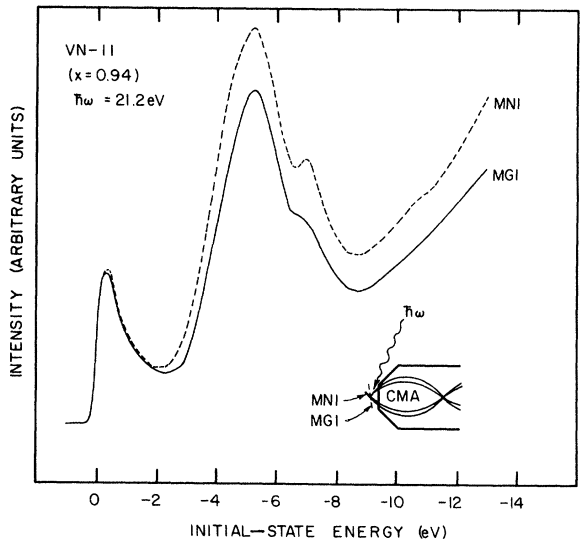

FIG. 8. Photoemission EDC's at $\hbar\omega = 21.2$ eV showing the residual angular dependences of the structure between − 4.0 and − 8.0 eV. The meaning of "most normal incidence" (MNI) and "most grazing incidence" (MGI) are shown in the inset for the present context.

TABLE II. Electron-energy-loss values for VN_x samples. Loss values in eV.[a]

Sample	x	A	B	C	D	E	F	G	H	I
	0.76	3.3	7.6	10.9	14.5	21.6	25.6	39.3	45.7	68.0
		(0.1)	(0.2)	(0.2)	(0.2)	(0.2)	(0.2)	(0.6)	(0.3)	(0.4)
VN-5	0.80	2.9	7.0	10.8	15.5	21.1	25.3	39.9	46.0	68.0
		(0.1)	(0.1)	(0.1)	(0.1)	(0.3)	(0.1)	(0.1)	(0.2)	(0.1)
VN-6	0.84	2.9	6.9	10.8	15.5	21.1	25.3	39.6	45.6	68.0
		(0.1)	(0.2)	(0.1)	(0.1)	(0.1)	(0.1)	(0.1)	(0.2)	(0.1)
VN-7	0.85	2.8	7.0	10.7	15.3	20.9	25.0	39.7	45.6	68.0
		(0.1)	(0.2)	(0.1)	(0.1)	(0.2)	(0.2)	(0.1)	(0.3)	(0.1)
VN-9	0.92	2.9	6.9	10.8	15.3	21.1	25.2	39.8	46.1	68.1
		(0.1)	(0.1)	(0.1)	(0.3)	(0.2)	(0.2)	(0.2)	(0.3)	(0.2)
VN-10[b]	0.94	2.7	7.1	10.7	15.9	21.0	24.8	39.9	45.8	67.9
		(0.1)	(0.1)	(0.1)	(0.1)	(0.1)	(0.1)	(0.2)	(0.2)	(0.1)
VN-11	0.94	2.8	6.9	11.0	15.6	21.2	25.2	39.5	45.4	68.0
		(0.1)	(0.1)	(0.1)	(0.1)	(0.1)	(0.1)	(0.2)	(0.2)	(0.1)
VN-*F*6	0.96	2.9	7.2	10.9	14.9	21.0	25.3	39.3	45.4	67.6
		(0.1)	(0.1)	(0.1)	(0.2)	(0.1)	(0.2)	(0.1)	(0.2)	(0.2)

[a] The loss values reported are the average of several measurements. The standard deviation is given in parentheses.

[b] This sample showed approximately 5% V_2N in the x-ray diffraction pattern.

lar dependence of the hybridized region. Our experimental apparatus does not allow independent variation of the incidence and collection angles. The inset in Fig. 8 shows the meaning of "most normal incidence" (MNI) and "most grazing incidence" (MGI) in the present context. For all samples, the -5.2-eV and the -7.0-eV shoulder were better resolved at MNI, while the bandwidth remained the same. From our data alone, one can only speculate about the origin for this angular dependence. Actual angular dispersion is possible since the CMA does not integrate over all emission angles and the samples showed grains (1–2 mm) larger than the light-beam width.

Figure 9 shows EDC's from samples of several compositions for $\hbar\omega = 21.2$ eV. Peak and minima locations are tabulated in Table III. No simple rigid-band-like shifts are observed in either the peak locations or the bandwidth. There is only a slight hint of the shoulder at -7.0 eV in the $VN_{0.76}$ sample (and this was not angle related). The largest peak lies 0.3–0.4 eV deeper in the $VN_{0.76}$ sample than in the $VN_{0.92}$ sample. This is actually reversed from a rigid-band expectation. These results seem to imply a more complicated rearrangement of the hybridized bands as x increases and are supported by results at $\hbar\omega = 16.8$ eV.

V. CONCLUSIONS

To our knowledge, there are no previous ELS results on any of the TMNC's with which we can

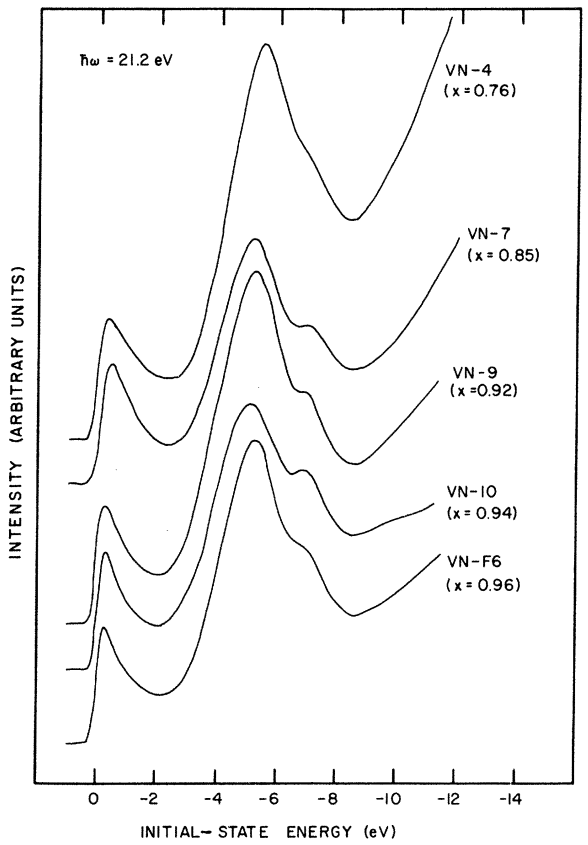

FIG. 9. Photoemission EDC's at $\hbar\omega = 21.2$ eV for δ-VN samples of several compositions. The spectra are normalized with respect to the peak near E_F.

TABLE III. UPS results for $\hbar\omega = 21.2$ eV.

Sample	x	EDC	Peaks	(eV)	EDC minima (eV)	Hybridized bandwidth (eV)
VN-4	0.76	−0.3	−5.5		−2.3	8.3
VN-5	0.80	−0.3	−5.5	−6.9	−2.2	8.5
VN-6	0.84	−0.3	−5.5	−6.9	−2.3	8.3
VN-7	0.85	−0.4	−5.2	−7.0	−2.3	8.5
VN-9	0.92	−0.2	−5.2	−6.9	−2.2	8.5
VN-10	0.94	−0.3	−5.1	−6.8	−2.1	8.5
VN-11	0.94	−0.3	−5.2	−7.0	−2.1	8.5
VN-*F*6	0.96	−0.2	−5.2	−6.8	−2.0	8.5
Ref. 10	1.00	E_F	−5.8	−7.0	−2.7	8.7

compare our data. Loss functions for TiC_x calculated from optical work by Lynch *et al.*[21] show many of the same general features as our VN_x results: (1) a peak in the volume-loss function near the calculated free-electron plasmon energy, and (2) a lowered plasmon peak of unknown microscopic origin. The optical results do not show the sharp low-energy peak, but this is understandable in that reflection ELS experiments are known to violate the dipole selection rules governing optical work. Our previous work with pure transition metals[27] has demonstrated the reliability of our methods and we have taken adequate precautions to avoid errors due to surface or bulk contamination by oxygen, carbon, or other contaminants.

The UPS results indicate good qualitative agreement with the calculated DOS of Neckel *et al.*[10] The experimental peak and minima positions lie slightly closer to E_F than predicted, but the bandwidth (8.5 eV) is in good agreement. While there are no other UPS results on δ-VN with which to compare our data, recent work by Johansson *et al.*[19] on the very similar material, TiN, appears to reveal much the same type of structure.

Neither the ELS nor UPS results indicate rigid-band-like behavior as the N/V ratio changes. This is contrary to models used recently to explain neutron scattering data on VN_x (Ref. 34) and the assumptions made by Rietschel *et al.*[35] in their discussion of the role of paramagnons in superconductivity in VN. Our observations are in basic agreement with previous experimental work on compositional dependence of the electronic structure of TiC_x.[16,21] Theoretical work on this problem has been carried out by several groups[36-39] but little agreement has been found. Our experimental results seem to imply a more complicated rearrangement of the hybridized bands with changes in N/V. Some of the general predictions of Klima[39] in regard to TiC_x seem to be borne out in the VN_x results, namely the loss of fine structure and the shift of the second major valence-band peak to greater binding energy as x decreases.

Improvements on this VN_x work could be made by expanding the photon-energy range used for UPS measurements in order to further study photon-energy dependences of the EDC's. Synchrotron radiation is ideal for this purpose, but the involved sample preparation and cleaning procedures that we have found necessary with VN are rather inconvenient for synchrotron work. Of course, angle-resolved studies on single crystals would help determine energy-band dispersions, but sample-related problems are likely to be even more severe. We have started similar work on NbN_x and ZrN_x. Preliminary results are quite similar to those reported here for VN and are planned to be published in a later paper.

ACKNOWLEDGMENTS

The Ames Laboratory is operated for the U. S. Department of Energy by Iowa State University under Contract No. W-7405-Eng-82. This research was supported by the Director for Energy Research, Office of Basic Energy Sciences under Grant No. WPAS-KC-02-02-02.

[1] L. E. Toth, *Transition Metal Carbides and Nitrides* (Academic, New York, 1971), Vol. 7.
[2] W. S. Williams, in *Progress in Solid State Chemistry*, edited by M. Reiss and J. D. McCalden (Pergamon, New York, 1971), Vol. 6.
[3] E. K. Storms, *The Refractory Carbides* (Academic, New York, 1967), Vol. 2.
[4] V. Ern and A. C. Switendick, Phys. Rev. 137, A1927 (1965).
[5] R. G. Lye and E. M. Logothetis, Phys. Rev. 147, 622 (1966).
[6] J. B. Conklin, Jr. and D. J. Silversmith, Int. J. Quan-

tum Chem. 2S, 243 (1968).
[7]H. R. Trebin and H. Bross, J. Phys. C 8, 1181 (1975).
[8]K. Schwarz, J. Phys. C 8, 809 (1975).
[9]J. F. Alward, C. Y. Fong, M. El-Batanouny, and F. Wooten, Phys. Rev. B 12, 1105 (1975).
[10]A. Neckel, P. Rastl, R. Eibler, P. Weinberger, and K. Schwarz, J. Phys. C 9, 579 (1976).
[11]A. L. Ivanovskii, V. A. Gubanov, E. Z. Kurmayev, A. L. Hagström, S. E. Karlsson, and L. I. Johansson, J. Electron Spectrosc. Relat. Phenom. 16, 415 (1979).
[12]K. Schwarz, J. Phys. C 10, 195 (1977).
[13]M. Gupta and A. J. Freeman, Phys. Rev. B 14, 5205 (1976).
[14]J. L. Calais, Adv. Phys. 26, 847 (1977).
[15]L. I. Johansson, A. L. Hagström, B. E. Jacobson, and S. B. M. Hagström, J. Electron Spectrosc. Relat. Phenom. 10, 259 (1977).
[16]A. L. Hagström, L. I. Johansson, S. B. M. Hagström, and A. N. Christensen, J. Electron Spectrosc. Relat. Phenom. 11, 75 (1977).
[17]J. F. Alward, C. Y. Fong, M. El-Batanouny, and F. Wooten, Solid State Commun. 17, 1063 (1965).
[18]A. L. Hagström, L. I. Johansson, B. E. Jacobson, and S. B. M. Hagström, Solid State Commun. 19, 647 (1976).
[19]L. I. Johansson, P. M. Stefan, M. L. Shek, and A. N. Christensen, Phys. Rev. B 22, 1032 (1980).
[20]J. H. Weaver, A. M. Bradshaw, J. F. van der Veen, F. J. Himpsel, D. E. Eastman, and C. Politis, Phys. Rev. B 22, 4921 (1980).
[21]D. W. Lynch, C. G. Olson, D. J. Peterman, and J. H. Weaver, Phys. Rev. B 22, 3991 (1980).
[22]G. Brauer and W. D. Schnell, J. Less-Common Met. 6, 326 (1964).
[23]H. Hahn, Z. Anorg. Allg. Chem. 258, 58 (1949).
[24]L. E. Toth, C. P. Wang, and C. M. Yen, Acta Metall. 14, 1403 (1966).
[25]N. Pessall, R. E. Gold, and H. A. Johansen, J. Phys. Chem. Solids 28, 333 (1967).
[26]F. I. Ajami and R. K. MacCrone, J. Phys. Chem. Solids 36, 7 (1975).
[27]W. K. Schubert and E. L. Wolf, Phys. Rev. B 20, 1855 (1979).
[28]J. E. Rowe, S. B. Christman, and E. E. Chaban, Rev. Sci. Instrum. 44, 1675 (1973).
[29]T. V. Vorburger, B. J. Waclawski, and D. R. Sandstrom, Rev. Sci. Instrum. 47, 501 (1976).
[30]R. E. Dietz, E. G. McRae, and J. H. Weaver, Phys. Rev. B 21, 2229 (1980).
[31]L. C. Davis and L. A. Feldkamp, Solid State Commun. 19, 413 (1976).
[32]J. H. Weaver, D. W. Lunch, and C. G. Olson, Phys. Rev. B 10, 501 (1974).
[33]J. H. Weaver, D. W. Lynch, and C. G. Olson, Phys. Rev. B 7, 4311 (1973).
[34]W. Weber, P. Roedhammer, L. Pintschovius, W. Reichardt, F. Gompf, and A. N. Christensen, Phys. Rev. Lett. 43, 868 (1979).
[35]H. Reitschel, H. Winter, and W. Reichardt, Phys. Rev. B 22, 4284 (1980).
[36]A. Neckel, P. Rastl, K. Schwarz, and R. Eibler-Mechtler, Z. Natuforsch. Teil A 29, 107 (1974).
[37]J. Zbasnik and L. E. Toth, Phys. Rev. B 8, 452 (1973).
[38]G. Reis and H. Winter, J. Phys. F 10, 1 (1980).
[39]J. Klima, J. Phys. C 12, 3691 (1979).